International Journal of Engineering

Journal Homepage: www.ije.ir

Fe/TiO_2 Catalyst for Photodegradation of Phenol in Water

F. Akhlaghian*, S. Sohrabi

Department of Chemical Engineering, Faculty of Engineering, University of Kurdistan, Sanandaj, Iran

PAPER INFO

Paper history:
Received 06 November 2014
Received in revised form 01 January 2015
Accepted 13 March 2015

Keywords:
Nanostructured
Photocatalysis
Titania
Phenol Degradation
Catalyst Coating

ABSTRACT

In this work, Fe/ TiO_2 nanostructured catalyst was prepared using the sol-gel method developed by Yoldas and tested for degradation of phenol in water under UV radiation. The synthesized catalyst was characterized by XRF; XRD; specific surface area, and porosimetry; and SEM methods. SEM results confirmed the nano dispersion of iron oxides on titania support. Effects of Fe load of the catalyst, dosage of the catalyst, pH, H_2O_2 amount, and time were investigated. Results of phenol photodegradation over Fe/TiO_2 showed that the reaction followed an apparent first order kinetics at low phenol concentration, and apparent rate constant was 0.0017 min^{-1}. Also, there was an optimum for Fe load of the catalyst. The better photocatalytic activity of Fe/TiO_2 coated on leca particles was observed in comparison to Fe/TiO_2 powder.

***doi**: 10.5829/idosi.ije.2015.28.04a.02*

1. INTRODUCTION

Over many years, the world health organization (WHO) has reported insufficient drinking water; on the other hand, developing industries discharge huge volume of wastewater into water sources and make them increasingly contaminated. Chemical industries which produce dyes, pesticides, and drugs are specifically responsible for this contamination as they discharge phenol and its derivatives, containing high toxic and carcinogenic compounds into water. Phenol is detrimental to human health, so the environmental protection agency (EPA) has limited the phenol concentration to less than 1 ppb [1-6]. Moreover, for sustainability of water resources, wastewater treatment issues have gained momentum during the recent decades [7, 8].

The most widely used methods for removal of phenolic compounds from water are adsorption and chemical oxidation. Adsorption refers to the transfer of pollutant from aqueous to solid phase; however, it is not a permanent method since the adsorbent needs to be regenerated. Photocatalytic oxidation has recently been proposed as an effective and economical method of converting pollutants into carbon dioxide and water [2, 9]. Phenol photodegradation can be explained by the advanced oxidation process (AOP) promoted by heterogeneous photocatalytic conversion of contaminant organic material to nontoxic materials i.e. CO_2 and H_2O. First, as a result of UV radiation, photons with energies higher than the band gap of the semiconductor materials like TiO_2 excite the electron valence band, then the excited electron migrates to the conduction band and a hole (h^+) is produced. The generated electron (e^-) and the hole (h^+) are strong oxidizing and reducing agents, respectively. Holes react with H_2O and OH^- to produce $\cdot OH$, O_2^-, and HO_2^- radicals. The generated radicals oxidize the contaminant organic materials into CO_2 and H_2O [10, 11]. When the reduction and oxidation reactions do not proceed simultaneously, an electron accumulation occurs in the conduction band which causes the rate of the recombination of e^- and h^+ to increase. The recombination causes energy dissipation that should be prevented to ensure efficient photocatalysis [11].

Titanium dioxide has the potential to be applied in the decomposition of many organic pollutants due to its optical and electrical properties, low cost, chemical stability, and nontoxicity [12]. TiO_2 with a modified

*Corresponding Author's Email: Akhlaghianfk@gmail.com (F. Akhlaghian)

morphology including nanotubes, foams, mesoporous phases, etc. has shown improved photocatalytic behaviors. The photo activity is strongly dependent on its crystalline structure, crystallite size, surface morphology, and synthesis method [8].

Recently, considerable efforts have been made to develop TiO_2 catalyst to improve their catalytic behaviors. Hung et al. [13] synthesized TiO_2 and Fe-TiO_2 by the sol-gel method and tested their photocatlytic activity for dichloromethane degradation in the gaseous phase. The effects of two types of oxidant agents in water, oxygen, and hydrogen peroxides with nanosized iron-doped anatase TiO_2 catalysts were investigated by Adan et al. [14]. Lorret et al. [12] tested the activity of $Ti(W)O_x$ sol-gel photocatalyst under ultraviolet light for photodegradation of methylene blue and found that the catalyst activity depends on the tungsten content and precursor choice. Shawabkeh et al. [15] evaluated the photocatalytic activity of Fe-TiO_2 catalyst for phenol degradation using visible light irradiation from sun, UV light source, and dark environment. Khraishel et al. [16] showed that undoped TiO_2 and Cu doped TiO_2 have high efficiency for phenol degradation. Palaismy et al. [17] synthesized mesopore Fe_2O_3/TiO_2 by sol-gel method and applied it for photocatalytic degradation of 4-chlorophenol under visible light radation. Crişşan et al. [18] prepared Fe-doped sol-gel TiO_2 nanopowder and investigated its structure, magnetic properties, and its photocatalytic activity for degradation of nitrobenzene in water. Oros-Ruiz et al. [19] investigated the effect of Au, Ag, Cu, and Ni nano particles deposited on TiO_2 and applied them for photodegradation of trimethoprim.

Various methods are available for preparation of the photocatalysts. Among them sol-gel methods are found appealing. They have benefits such as synthesis of nano-sized crystallized powder at low temperature, preparation of composite materials, possibility of stoichiometry controlling of process, and coating surfaces with different types and shapes [20, 21].

In this work, nanostructured Fe/TiO_2 photocatalyst was synthesized by the sol-gel method developed by Yoldas and tried to use the easy coating property of this method [21]. The photocatalyst was characterized and its photo activity was investigated. The photo catalyst was also coated on leca particles. The photocatalytic activity of coated and powder form catalysts was compared.

2. MATERIALS AND METHODS

2. 1. Materials Titanium isopropoxide and $Fe(NO_3)_3.9H_2O$ were used as precursors for titania and Fe, respectively. Ethanol, nitric acid, H_2O_2, and phenol were also used. All the materials were of analytical grade, used without further purifications, and purchased from Merck Company. Double-distilled water was used throughout the experiments.

2. 2. Synthesis of Fe/TiO$_2$ Following Yoldas method, titanium isopropxide was added to the double-distilled water. The molar ratio of titanium isopropoxide to water was 1:100. The mixture was stirred at a constant rate at 85°C for 45 min. The nitric acid was added. The molar ratio of titanium isopropoxide to nitric acid was 1:0.07. $Fe(NO_3)_3.9H_2O$ was dissolved in ethanol and a solution of Fe 2wt.% was obtained. Fe was added to the mixture through this solution. The mixture was stirred at a constant rate at 85°C for 24 h. The obtained gel was dried at 100°C in an oven for 12 h. Finally, the dried gel was calcined in a muffle furnace at 600°C for 2 h. The Fe/TiO_2 powder was crushed and sieved into 60-90 μm particles. Leca particles sized 4-10 mm were used as the substrate for coating by the catalyst. The gel mixture stirred at 85°C for 24 h was used for coating. The leca particles were immersed in the gel mixture and coated by dip coating method. The coated leca particles were dried at 100°C for 12 h and calcined at 600°C for 2 h.

2. 3. Characterization Iron content of the catalyst was measured by Spectro X-ray fluorescence (XRF) spectrometer. The degree of crystalline order of the sample was assessed via X-ray diffraction (XRD) using X'pert MPD diffractometer with Co K_α radiation at 40 kV and 40 mA. The XRD patterns were collected from 5-80° in 2θ at a scan rate of 0.2°/s. The specific surface area and porosity were obtained using Micrometrics ASAP 2010. Before measuring nitrogen adsorption, the catalyst was degassed at 300°C for 6 h. The structure and morphology of the catalyst was investigated by field emission scanning electron microscopy of FESEM of TESCAN Company. UV-Vis spectrometer Specord 210 was used for measuring phenol concentration in water.

2. 4. Photocatalysis Experiments The setup, as shown in Figure 1, consisted of batch Pyrex reactor illuminated by a UV lamp with peak intensity of 254 nm, fixed 19.5 cm above the reactor center. The system was in a chamber shielded by aluminum foil during the reaction to prevent the outside light interference. First, 0.1 g of Fe/TiO_2 catalyst was added to 200 ml of phenol solution in water which was used as wastewater. Then, 12.5 ml of hydrogen peroxide (30 wt.%) was added to the solution. The mixture was transferred to the reactor and stirred at a constant rate under UV lamp (Light intensity was 242.35 or 757.28 W/m^2) for 2 h. All the experiments were carried out at room temperature

(20°C). Then, the mixture was centrifuged, and the absorbance of the supernatant solution was measured at 270 nm using a Specord 210 UV spectrometer. The experiments were replicated with a blank. All the conditions in the blank were the same as those of the sample except the blank had no catalyst. The concentration of phenol in the solution was measured using Beer-Lambert law, and the photodegradation was calculated using the following equation [22]:

$$\text{Degradation}\ \% = 100 \times \left[\frac{(A_0-A)}{A_0}\right] \quad (1)$$

where A_0 and A are absorbance of the blank and the sample, respectively. Each experiment was repeated three times, and the average is reported. The standard deviations for all the experiments are less than 0.06.

3. RESULTS AND DISCUSSION

3. 1. Optimum Fe Load Since the photo activity of Fe/TiO_2 is highly affected by Fe load, preliminary experiments were done to distinguish the catalyst with optimum Fe load. Fe/TiO_2 photocatalysts were synthesized with different Fe loads and called A, B, C, D, and E. The catalysts were analyzed by an X-ray fluorescence (XRF), and their chemical analyses were determined. The catalysts A, B, C, D, and E were pure titania, 0.2% Fe_2O_3/TiO_2, 0.27% Fe_2O_3/TiO_2, 0.41% Fe_2O_3/TiO_2, and 0.5%Fe_2O_3/TiO_2, respectively. Figure 2 shows that catalyst C, 0.27%Fe_2O_3/TiO_2 had the best phenol degradation yield. Thus, it was chosen as the best catalyst, and used for characterization and activity tests.

3. 2. Mechanism When Fe/TiO_2 is illuminated by UV light, the electron of TiO_2 valence band transfers to Fe^{3+} and causes a reduction from Fe^{3+} to Fe^{2+}. The generated hole in the valence band can produce hydroxyl radicals, and subsequently •OH radical oxidizes the organic material to CO_2 and H_2O. The generated Fe^{2+} can produce superoxide radical (O_2^-) [10, 11]. Fe^{3+} consumes photo electron and decreases the recombination reaction rate of h^+ and e^-, so the activity of the photocatalytic reaction is improved. When the Fe load exceeds the optimum amount, Fe may act as recombination center and this is unfavorable for photocatalysis reaction [11].

3. 3. Characterization

3. 3. 1. XRD XRD pattern of catalyst A (pure titania) and catalyst C (0.27%Fe_2O_3/TiO_2) are shown in Figure 3. The XRD patterns of pure titania with peaks at 32.0095°, 42.1696° were attributed to the rutile phase (JCPDS File no. 21-1276), and smaller peaks at 29.5090°, 44.2294°, and 56.4824° were attributed to anatase (JCPDS File no. 21-1272). These results imply that both rutile and anatase phases existed in pure titania. In XRD pattern of Fe/TiO_2, in addition to peaks belonging to rutile and anatase phases (JCPDS Files no. 21-1276), other peaks were also identified which corresponded to iron oxides Fe_2O_4 (JCPDS File no. 19-0629), and Fe_2O_3 (JCPDS File no. 39-1346). The anatase weight percent can be calculated by [23, 24]:

$$X_A(\%) = \frac{100}{1+1.26(I_R/I_A)} \quad (2)$$

where X_A denotes the weight fraction of anatase; I denotes the intensity of the strongest reflection; and the subscripts A and R denote the anatase and rutile phases, respectively. Crystallite size is estimated by Scherrer formula [23]:

$$D = k\lambda/(\beta.\cos\theta) \quad (3)$$

where D is the crystallite size (nm), k is a correction factor taken as 0.89, λ is the wave length of X-radiation (Co k_α=0.178897 nm), β is the full width at half maximum peak, and θ is the diffraction angle. The average crystallite size must be estimated considering both anatase and rutile peaks according to the following relationship [23]:

$$D_{ave} = \frac{D_A I_A + D_R I_R}{I_A + I_R} \quad (4)$$

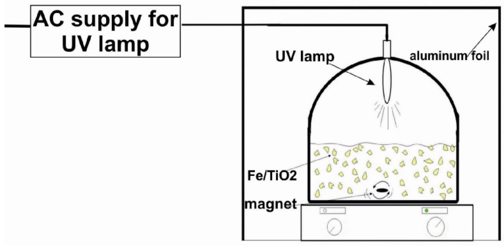

Figure 1. Schematic representation of the setup

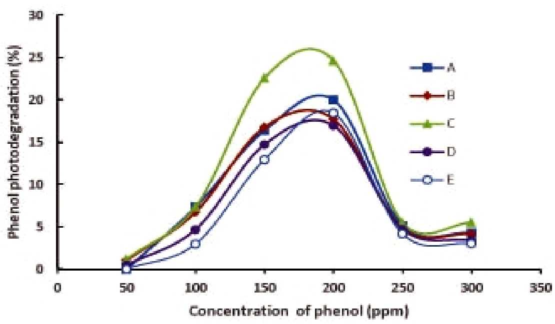

Figure 2. The effect of initial concentration on the phenol photodegradation for the catalysts A, B, C, D, and E (intensity of UV radiation was 242.36 mW/cm^2)

D_A and D_R are crystallite sizes of anatase and rutile phases, respectively. The degree of crystallinity is given by [25]:

$$C = 100 \times \frac{I_C}{I_C + I_{Am}} \quad (5)$$

where C is the degree of crystallinity; I_C and I_{Am} are the intensities of X-ray scattered by crystalline and amorphous regions, respectively. Table 1 shows the percentages of rutile and anatase phases, the crystalline size, and the degree of crystallinity. As it is seen, more than 90% of titania crystals were in the rutile phase. Also, addition of Fe reduced the crystalline size and the degree of crystallinity [23, 24]. Crystallinity is reduced as the dopant is introduced into the lattice. It originates from the fact that the order of TiO_2 lattice is distributed by the dopant due to the different atom sizes of Fe^{3+} and Ti^{4+}.

3. 3. 2. Porosimetry Nitrogen adsorption/desorption isotherm of 0.27% Fe_2O_3/TiO_2 catalyst is shown in Figure 4(A). The isotherm shape showed that the Fe/TiO_2 catalyst was mesoporous and according to the IUPAC classification, nitrogen adsorption/desorption was type IV and its hysteresis was type H2. Catalysts with H2 type hysteresis have ink-bottle pores (small body and large mouth) [26]. Pore size distribution is shown in Figure 4(B), and is multimodal. The prevalence of the pores decreases as pore diameter increases. Table 2 shows specific surface area, average pore diameter, and pore volume of the catalyst, calculated using Barrett-Joyner-Halenda (BJH) desorption method.

3. 3. 3. SEM The SEM images of the Fe/TiO_2 catalyst are given in Figure 5. Images a and b show that the particles did not have any particular shape and they were not uniform in size. The brilliant spots of image c were related to nano size iron oxide particles dispersed in titania support.

TABLE 1. Textural characteristics of TiO_2 and Fe/TiO_2

Samples	Anatase (wt. %)	Rutile (wt. %)	Crystallite size (nm)[b]	Degree of crystallinity (%)[b]
TiO_2	9.03	90.97	57.03	81.21
Fe/TiO_2	5.41	94.59	50.93	73.32

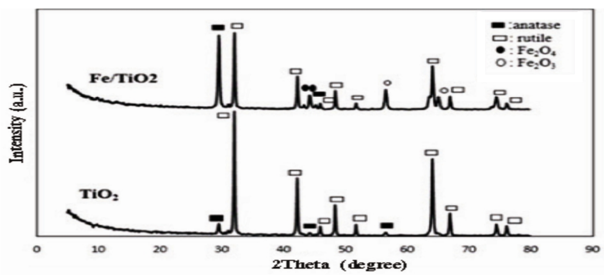

Figure 3. XRD patterns of TiO_2 and Fe/TiO_2

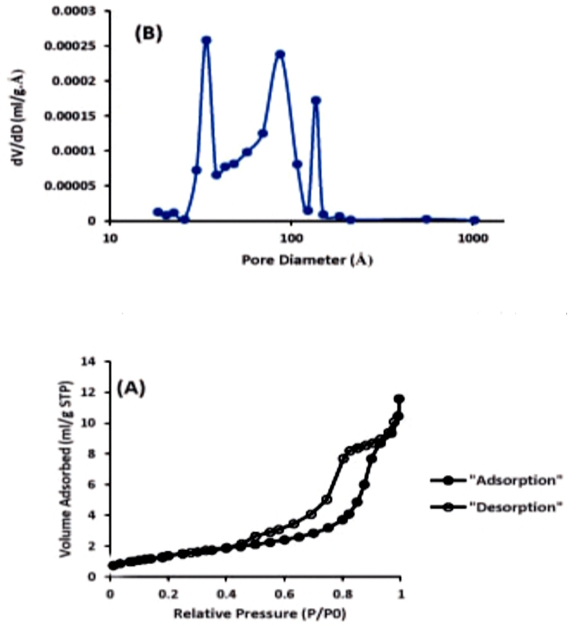

Figure 4. (A) Liquid nitrogen adsorption/desorption isotherm of Fe/TiO_2 catalyst and (B) pore size distribution in accordance with BJH desorption of Fe/TiO_2 catalyst

TABLE 2. The specific surface area, average pore volume, and average pore diameter of the Fe/TiO_2 catalyst

Surface area ($m^2 g^{-1}$)	Average pore volume ($cm^3 g^{-1}$)	Average pore diameter (nm)
8.2873	0.017980	86.782

BET and pore volume are calculated from the BJH desorption isotherm (average diameter is calculated with 4V/S and S is considered the pore surface area).

3. 4. Photocatalytic Activity

3. 4. 1. Initial Concentration Figure 1 shows the effect of phenol initial concentration on phenol degradation for all the catalysts from A to E. In the phenol concentration range of 50-200 ppm, degradation increased with an increase in phenol concentration, but at concentration greater than 200 ppm, phenol degradation decreased with an increase in initial concentration of phenol due to the occupation of catalyst active sites by molecules and insufficient ·OH radicals for phenol photodegradation [22, 27, 28]. According to Figure 1, these trends are similar for all the catalysts from A to E.

3. 4. 2. Catalyst Dosage Degradation of phenol with photocatalyst dosage is represented in Figure 6. First, phenol degradation was raised with increasing dosage of the photocatalyst due to an increase in the number of the photocatalyst active sites. When dosage of the photocatalyst increased to greater than 0.5 g/L, phenol degradation decreased because of the increase in the opacity of the suspension and scattering of the light as it could not penetrate to the depth, and few sites of the catalyst were activated [22, 28].

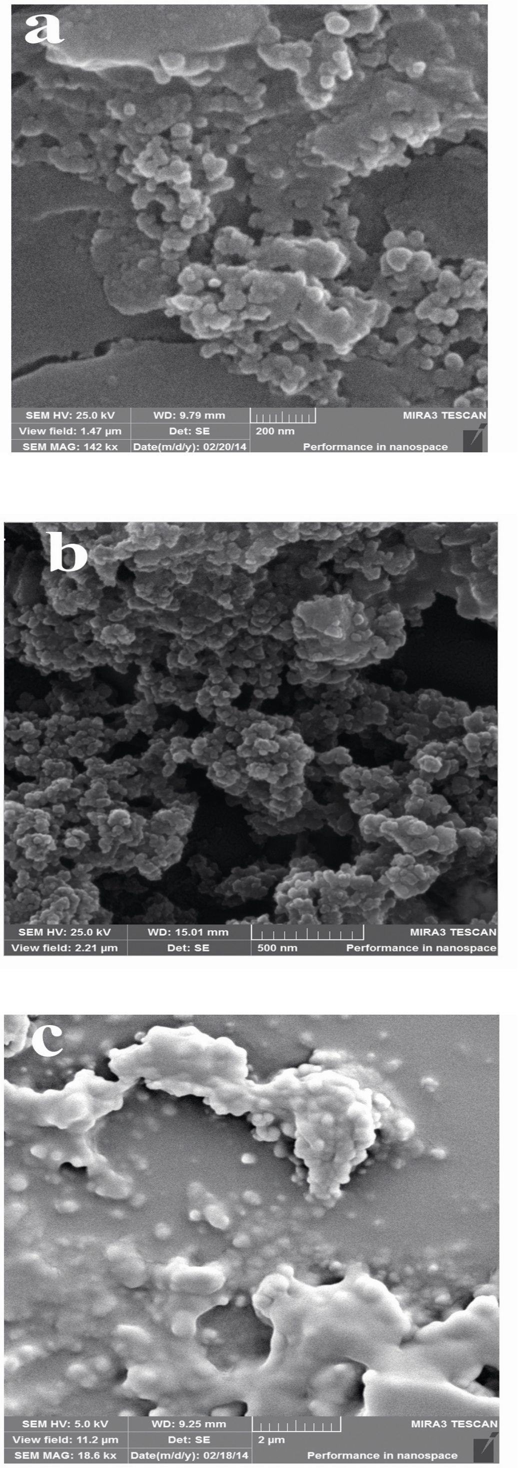

Figure 5. SEM images of the Fe/TiO_2

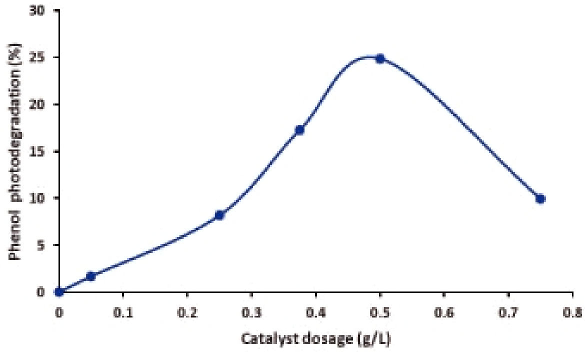

Figure 6. Effect of the photocatalyst dosage on the degradation of phenol (intensity of UV radiation was 757.38 mW/cm^2, and phenol initial concentration was 200 ppm)

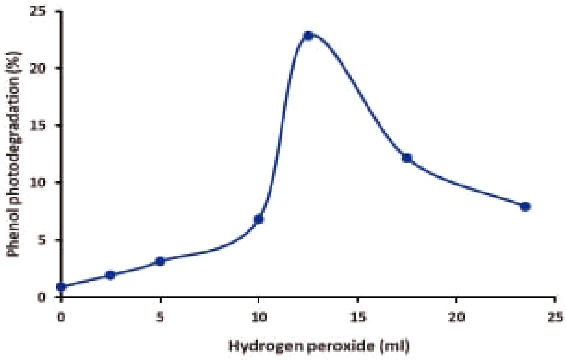

Figure 7. Effect of H_2O_2 (30 wt.%) on the phenol photodegradtion (intensity of UV radiation was 757.38 mW/cm^2, and phenol initial concentration was 200 ppm)

3. 4. 3. H_2O_2 Hydroxyl radicals were produced upon photolysis of H_2O_2 in the presence of UV radiation. Hydroxyl radical is an electron acceptor which avoids electron-hole recombination and reacts with phenol [5, 10]. At low H_2O_2 concentration, H_2O_2 cannot produce enough ·OH radicals, so phenol photocatalytic degradation is small [5, 10]. At high hydrogen peroxide concentration, ·OH radicals react with H_2O_2 in excess. This reaction consumes hydroxyl radicals and competes with phenol oxidation. A decrease in hydroxyl radical concentration also causes phenol photocatalytic degradation to decrease. Figure 7 shows the phenol degradation with the amount of H_2O_2 (30 wt.%). As shown, the optimum amount for H_2O_2 (30 wt.%) was 12.5 ml.

3. 4. 4. pH The maximum photocatalytic degradation of phenol was observed at pH=9 as shown in Figure 8. In the acidic pH, there were competitions between the phenol and anions of the solution for reaction with ·OH and also the catalyst active sites which reduced phenol degradation [29]. At pH>9, high concentration of OH^- resulted in deactivation of ·OH. The reaction between OH^- and ·OH produced H_2O_2 and

•OH_2. The reaction between ·OH_2 with phenol was also very low. At high pH, more radical-radical reactions occurred and reduced the phenol degradation [29]. The optimum pH for photocatalytic degradation which was determined experimentally was 9.

3. 4. 5. Kinetic Model Many kinetic models for the photocatalytic decomposition of organic contaminants in water have been reported [5, 23]. Langmuir-Hinshelwood (L-W) is a model commonly applied for heterogeneous photocatalytic reactions:

$$r = -\frac{dC}{dt} = k\left(\frac{KC}{1+KC}\right) \tag{6}$$

where r is the rate of reaction (ppm/min), k is the photocatalysis rate constant (ppm/min), K is the adsorption rate constant (ppm^{-1}) and C is the contaminant concentration (ppm) [5, 23]. At low concentration (KC≤1), KC is negligible compared to 1, and the reaction rate follows an apparent first order kinetic model. Integration of Equation (2) under these assumptions give:

$$-\ln\left(\frac{C}{C_0}\right) = k_{app}t \tag{7}$$

where C_0 is the initial concentration of organic contaminant and k_{app} is the apparent constant.

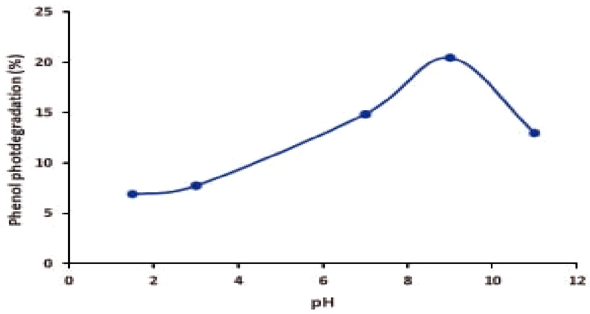

Figure 8. Effect of pH on the photocatalytic degradation of phenol (intensity of UV radiation was 757.38 mW/cm^2, and phenol initial concentration was 200 ppm)

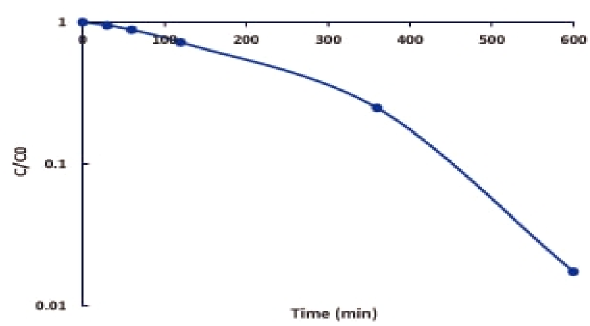

Figure 9. Phenol concentration with time (intensity of UV radiation was 757.38 mW/cm^2, and phenol initial concentration was 200 ppm)

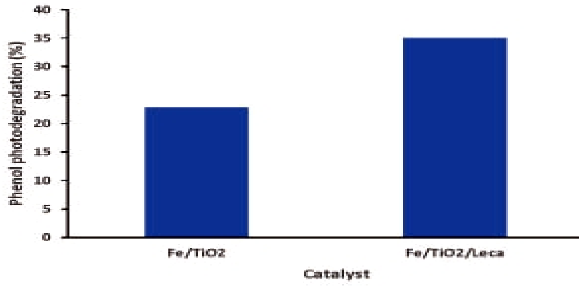

Figure 10. Effect of coating on photocatalytic activity (intensity of UV radiation was 757.38 mW/cm^2, and phenol initial concentration was 200 ppm)

TABLE 3. Apparent rate constant for photocatalytic degradation of phenol

Sample	Phenol degradation after 10 h	Apparent rate constant (min^{-1})	R^2
Fe/TiO_2 catalyst	98.26	0.0017	0.9751

Figure 9 shows that the photocatalytic degradation of phenol follows the apparent first order kinetic model. The apparent constant is calculated and reported in Table 3.

3. 4. 6. Fe/TiO_2/Leca Photocatalytic Activity Figure 10 shows the result of Fe/TiO_2/Leca photocatalytic activity. The dose of photocatalyst powder and Fe/TiO_2 coated on leca particles were the same, equal to 0.5 g/L. The better performance of Fe/TiO_2/Leca is obvious. Coating leca particles by Fe/TiO_2 increased the available surface area for photocatalytic reaction, and therefore improved the photocatalytic activity.

4. CONCLUSION

Fe/TiO_2 catalyst was synthesized using sol-gel method developed by Yoldas and successfully applied for the photocatalytic degradation of phenol in water. The optimum load for Fe was determined and the analysis of the catalyst was determined by XRF: 0.27% Fe_2O_3/TiO_2. The catalyst was characterized by XRD, specific surface area and porosimetry, and SEM techniques. The result of XRD showed that both Fe_2O_3 and Fe_2O_4 iron oxides existed in the catalyst. SEM images showed the nano size iron oxides particles on titania support. It is worth mentioning that the kinetic model of the reaction was apparent first order. Effects of the operating conditions of photocatalysis reaction including initial concentration of phenol in the solution, catalyst dosage, amount of H_2O_2, time, and pH were investigated and optimized. Fe/TiO_2 catalyst was coated on leca particles. The photocatalysis activity of Fe/TiO_2/Leca was better than Fe/TiO_2 powder due to its higher surface area. Finally, it was concluded that Fe/TiO_2 catalyst synthesized by the sol-gel technique based on Yoldas method is a promising catalyst for phenol degradation and photocatalysis process.

5. REFERENCES

1. Kebria, M. and Jahanshahi M., "Nanofiltration membrane synthesized from polyethleneimine for removal of $MgSO_4$ from aqueous solution", ***International Journal of Engineering***, Vol. 27, No. 8, (2014), 1173-1178.
2. Busca, G., Berardinelli, S., Resini, C. and Arrighi, L., " Technologies for the removal of phenol from fluid streams: A short review of recent developments", ***Journal of Hazardous Materials***, Vol. 160, No. 2-3, (2008), 265-288. .
3. Masomi, M., Ghoreyshi, A. A., Najafpour G.D. and Mohamed, A.R.B., "Adsorption of phenolic compounds onto activated carbon synthesized from pulp and paper mill sludge: equilibrium isotherm, thermodynamics, and mehanism studies", ***International Journal of Engineering***, Vol. 27, No. 10, (2014), 1485-1494..
4. Zareie, C. , Najafpour, G. and Sharifzadeh baei, M., "Preparation of nanochitosan as an effective sorbent for the removal of copper ions from aqueous solutions", ***International Journal of Engineering***, Vol. 26, No. 8, (2013), 829-836.
5. Cam, L.M., Khu, L.V. and Ha, N.N., "Theoretical study on the adsorption of phenol on activated carbon using density functional theory", ***Journal of Molecular Modeling***, Vol. 19, (2013), 4395-4402.
6. http://water.epa.gov/scitech/swguidance/standards/criteria/health/phenol_index.cfm (2014)
7. Poulopoulos, S.G., Arvanitaks, F. and Philippopoulos, C.J., "Photochemical treatment of phenol aqueous solutions using ultraviolet radiation and hydrogen peroxide", ***Journal of Hazardous Materials***, Vol. 129, No. 1-3, (2006), 64-68.
8. Lee, S.-Y. and Park, S.-J., "TiO_2 photocatalyst for water treatment applications", ***Journal of Industrial Engineering Chemistry***, Vol. 19, No. 6, (2013), 1761-1769.
9. Mathews, R.W., "Photocatalytic oxidation of organic contaminants in water: An aid to environmental preservation", ***Pure and Applied Chemistry***, Vol. 4, No. 9, (1992), 1285-1290.
10. Ahmed, S., Rasul, M.G., Martens, W.N., Brown R. and Hashib, M.A., " Heterogeneous photocatalytic degradation of phenols in wastewater: A review on current status and developments", ***Desalination***, Vol. 261, No. 1-2, (2010) 3-18.
11. Sun, L., Li, J., Wang, C.L., Li, S.F., Chen H.B. and Lin C.J., " An electrochemical strategy of doping Fe^{3+} into TiO_2 nanotubes array films for enhancement in photocatalytic activity", ***Solar Energy Materials and Solar Cells***, Vol. 93, No. 10, (2009), 1875-1880.
12. Lorret, O., Francovà, D., Waldner, G. and Stelzer, N., "W-doped totania nanoparticles for UV and visible-light photocatalytic reactions", ***Applied Catalysis B: Environmental***, Vol. 91, No. 1-2, (2009), 39-46.
13. Hung, W.-C., Fu, S.-H., Tseng, J.-J., Chu and H., Ko, T.-H., "Study on photocatalytic degradation of gaseous dichloromethane using pure and iron-doped TiO_2 prepared by the sol-gel method", ***Chemosphere***, Vol. 66, No. 11, (2007), 2142-2151.
14. Adan C., Carbajo, J., Bahamonde, A. and Martinez-Arias, A., "Phenol photodegradation with oxygen and hydrogen peroxide over TiO_2 and Fe-doped TiO_2", ***Catalysis Today***, Vol. 143, No. 3-4, (2009), 247-252.
15. Shawabkeh, R.A., Khashman, O.A. and Bisharat, G.I., "Photocatalytic degradation of phenol using Fe-TiO_2 by different illumination sources", ***International Journal of Chemisty***, Vol. 2, No.2, (2010), 10-18.
16. Khraisheh, M., Wu, L., Al-Muhtaseb, H.A., Albadarin, A.B. and Walker, G.M., "Phenol degradation by powdered metal ion modified titanium dioxide photocatalysts", ***Chemical Engineering Journal***, Vol. 213, (2012), 125-134.
17. Palanisamy, B., Babu, C., Sundaravel, B., Anandan, S. and Murugean, V., "Sol-gel synthesis of mesoporous mixed Fe_2O_3/TiO_2 photocatalyst: Application for degradation of 4-chlorophenol", ***Journal of Hazardous Materials***, Vol. 252-253, (2013), 233-242.
18. Crişan, M. , Răileanu, M., Drăran, N., Crişan, D., Ianculescu, A., Niţol, I., Oanccea, P., Şomăcescu, S, Stănică, N., Vasile, B. and Stan, C. "Sol-gel iron-doped TiO_2 nanopowders with photocatalytic activity", ***Applied Catalysis A: General***, in press (2015).
19. Oros-Ruiz, S., Zanella, R. and Prado B., " Photocatalytic degradation of trimethoprim by metallic nanoparticles supported on TiO_2-P25", ***Journal of Hazardous Materials***, Vol. 263, No. 1, (2013), 28-35.
20. Akpan, U.G. and Hameed, B.H., "The advancements in sol-gel method of doped-TiO_2 photocatalysts", ***Applied Catalysis A: General***, Vol. 375, No. 1, (2010), 1-11.
21. Brinker, C.J. and Scherer, G.W., "Sol Gel Science", New York, Academic Press, (1990).
22. Nezamzadeh-Ejhieh, A. and Salimi, Z., "Heterogeneous photodegradation catalysis of o-phenylenediamine using CuO/X zeolite", ***Applied Catalysis A: General***, Vol. 390, No. 1-2, (2010), 110-118.
23. McEvoy, J.G., Cui, W. and Zhang, Z., "Dgradative and disinfective properties of carbon-doped anatase-rutile TiO_2 mixtures under visible light irradiation", ***Catalysis Today***, Vol. 207, (2013), 191-199.
24. Nahar, M.S., Zhang, J., Hasegawa, K., Kagaya, S. and Kuroda, S., "Phase transformation of anatase-rutile crystals in doped and undoped particles obtained by the oxidation of polycrystalline sulfide", ***Materials Science in Semiconductor Processing***, Vol. 12, No. 4-5, (2009), 168-174.
25. Black, D.B. and Lovering, E.G., "Estimation of the degree of crystallinity in digoxin by X-ray and infrared methods", ***Journal of Pharmacy and Pharamcology***, Vol. 29, No. 11, (1977), 684-687.
26. Leofanti, G., Padovan, M., Tozzola, G. and Venturelli, B., " Surface area and pore texture of catalysts", ***Catalysis Today***, Vol. 41, No. 1-3, (1998), 207-219.
27. Shanker, M.V., Anandan, S., Venkatachalam, N., Arabindoo, B. and Murugesan, V., " Novel thin-film reactor for photocatalytic degradation of pesticides in an aqueous solution", ***Journal of Chemical Technology and Biotechnology***, Vol. 79, No. 11, (2004), 1279-1285.
28. Poretedal, H.R., Norozi, A., Keshavarz, M.H., and Semnani, A., "Nanoparticles of zinc sulfide doped with manganese, nickel and copper as nanophotocatalyst in the degradation of organic dyes", ***Journal of Hazardous Materials***, Vol. 162, No. 2-3, (2009), 674-681.
29. Liu, X., Tang, Y., Luo, S., Wang, Y., Zhang, X., Chen, Y., and Liu, C., " Reduced graphene oxides and $CuInS_2$ codecorated TiO_2 nanotubes arrays for efficient removal of herbicide 2,4-dichloropheoxyacetic acid from water", ***Journal of Photochemistry and Photobiology A: Chemistry***, Vol. 262, (2013), 22-27.

Fe/TiO_2 Catalyst for Photodegradation of Phenol in Water

F. Akhlaghian, S. Sohrabi

Department of Chemical Engineering, Faculty of Engineering, University of Kurdistan, Sanandaj, Iran

P A P E R I N F O

Paper history:
Received 06 November 2014
Received in revised form 01 January 2015
Accepted 13 March 2015

Keywords:
Nanostructured
Photocatalysis
Titania
Phenol Degradation
Catalyst Coating

چکیده

دراین کار، کاتالیست نانو ساختار Fe/TiO_2 با استفاده از روش سل-ژل ابداع شده بوسیله یولداس ساخته شد و در تجزیه فنل در آب تحت تابش UV آزمایش شد. کاتالیست سنتز شده بوسیله روش های XRF، XRD ، مساحت سطح ویژه و تخلخل سنجی، و SEM تعیین مشخصات شد. تخلخل سنجی ساختار مزوپور کاتالیست را نشان داد. نتایج SEM پراکندگی نانوذرات اکسیدآهن را بر روی پایه تیتانیا تایید کردند. اثرات بار آهن کاتالیست، مقدار کاتالیست، pH، مقدار H_2O_2 و زمان بررسی شدند. نتایج تجزیه فتو شیمیائی فنل برروی Fe/TiO_2 نشان داد که واکنش از سینتیک مرتبه اول پیروی می کند. ثابت سرعت ظاهری برابر با $۰/۰۰۱۷\ min^{-1}$ بود. همچنین مقداربهینه ای برای بار آهن کاتالیست وجود دارد. فعالیت فتوکاتالیستی بهتر Fe/TiO_2 پوشش داده شده برروی لیکا در مقایسه با Fe/TiO_2 پودری مشاهده شد.

***doi**: 10.5829/idosi.ije.2015.28.04a.02*